Accuracy of Breast Magnetic Resonance Imaging (MRI) and Breast Ultrasound Compared to Pathology in Assessing Residual Tumor in Breast Cancer Patients Receiving Neoadjuvant Systemic Treatment at Siriraj Hospital

Apinya Iamsamang, M.D.[1], Shanigarn Thiravit, M.D.[2], Voraparee Suvannarerg, M.D.[2], Pradit Rushatamukayanunt, M.D.[1], Pornpim Korpraphong, M.D.[2], Suebwong Chuthapisith, M.D.[1], Waraporn Imruetaicharoenchoke, M.D.[1,*]

[1]*Division of Head Neck and Breast, Department of Surgery, Faculty of Medicine Siriraj Hospital, Mahidol University, Bangkok 10700, Thailand,*
[2]*Division of Diagnostic Radiology, Department of Radiology, Faculty of Medicine Siriraj Hospital, Mahidol University, Bangkok 10700, Thailand.*

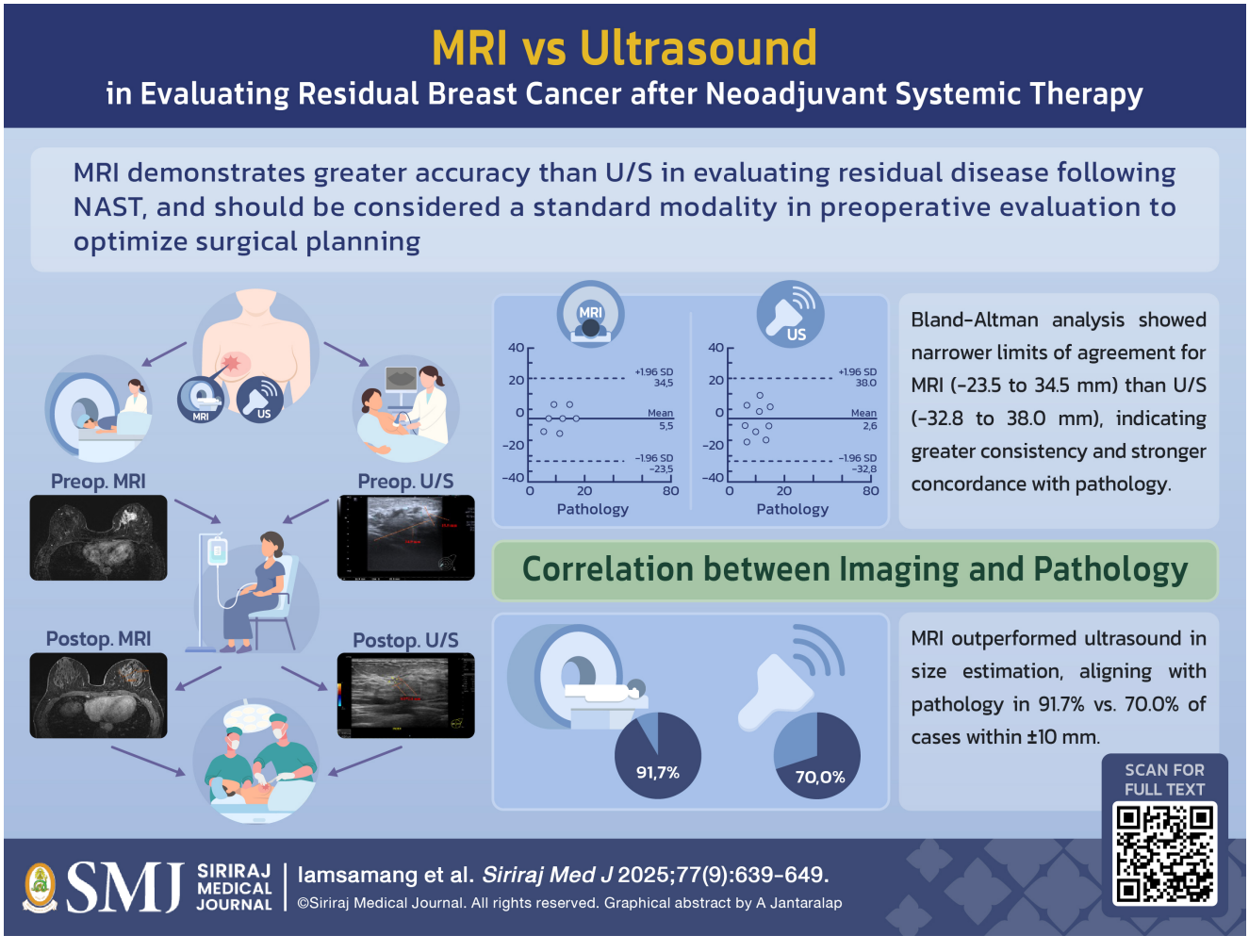

*Corresponding author: Waraporn Imruetaicharoenchoke
E-mail: Waraporn.imr@mahidol.ac.th
Received 23 June 2025 Revised 29 July 2025 Accepted 30 July 2025
ORCID ID:http://orcid.org/0000-0003-1566-5307
https://doi.org/10.33192/smj.v77i9.276157

ABSTRACT

Objective: To evaluate the accuracy of magnetic resonance imaging (MRI) and ultrasound (US) in assessing residual tumor size compared to pathological findings in breast cancer patients who received neoadjuvant systemic treatment (NAST), and to examine the influence of imaging on surgical planning across different molecular subtypes.

Materials and Methods: This retrospective study included 24 breast cancer patients who underwent NAST followed by surgery at Siriraj Hospital between 2016 and 2024. Preoperative breast MRI and breast US, performed within 3–6 weeks prior to surgery, were compared with pathological tumor size. Analysis focused on mass lesions, with non-mass enhancement (NME) considered in selected cases where it presented. Imaging findings were independently reviewed by a second, blinded radiologist. Concordance between imaging and pathology was assessed.

Results: A total 24 patients were analyzed. MRI showed superior agreement with pathological tumor size, with 91.7% of cases falling within a ±10 mm margin, compared to 70.0% for US. Mean tumor sizes were 5.4 mm for MRI, 8.3 mm for US, and 10.9 mm based on pathological examination. Bland-Altman analysis revealed better agreement between MRI and pathology (limits of agreement: –23.5 – 34.5 mm) compared to US. These results highlight the superior accuracy and reliability of MRI over US for preoperative tumor size assessment.

Conclusion: MRI demonstrates greater accuracy than US in evaluating residual disease following NAST. In case of invasive lobular carcinoma (ILC) subtypes, incorporating NME into imaging assessment may improve concordance with pathological findings. MRI should be considered a standard modality in preoperative evaluation to optimize surgical planning.

Keywords: Breast cancer; neoadjuvant chemotherapy; MRI; ultrasound; pathological concordance (Siriraj Med J 2025; 77: 639-649)

INTRODUCTION

Breast cancer is currently the most commonly diagnosed cancer among women, leading to rapid advancements in treatment strategies that markedly differ from those of the past.[1] This is particularly evident for tumors with high proliferative potential, leading to a high likelihood of lymphatic or distant metastasis, such as HER2-positive and triple-negative breast cancer (TNBC), and those with elevated Ki-67 expression.

In most cases, treatment begins with systemic therapy—including chemotherapy, targeted therapy, or immunotherapy—administered before surgery (neoadjuvant systemic treatment, or NAST). Systemic therapy may lead to a clinical complete response (cCR), characterized by the absence of detectable tumor on physical examination, mammography, and ultrasonography. In certain cases, a pathological complete response (pCR), defined as the absence of residual invasive cancer on histopathological assessment, may also be achieved, correlating with improved survival outcomes.[2]

The pattern of tumor shrinkage varies significantly.[3] According to a study by Erika M.S. et al., in patients with mass lesions visible on MRI, the correlation between MRI findings and final pathology was as high as 86%.[4] Most tumors presenting as mass lesions demonstrate concentric shrinkage mode (CSM) in response to NAST, which is more common in TNBC and HER2-positive subtypes. Conversely, tumors, especially the luminal subtype, exhibited on MRI as non-mass enhancement (NME) patterns tend to respond with a scattered shrinkage pattern.[5] These different patterns complicate post-NAST response assessment using mammography or US alone and may lead to positive surgical margins, necessitating reoperation and potentially compromising oncologic outcomes. In luminal tumors, concentric shrinkage is seen in only 45.7% of cases, compared to 66.2% in TNBC and 59% in HER2-positive cases.[6] Accurate preoperative imaging to determine the pattern of response after NAST is therefore critical in optimizing surgical planning and minimizing margin positivity, which is linked to increased local recurrence and reoperation.

MRI is the most sensitive modality for evaluating residual disease after NAST due to its superior contrast resolution and ability to detect NME or scattered tumor foci.[7] However, variability in MRI performance across molecular subtypes—overestimating or underestimating residual disease—highlights the need for further study.

While studies from Western countries and East Asia—including a recent large-scale Korean cohort study by Kim et al.[8]—have investigated the diagnostic accuracy of magnetic resonance imaging (MRI) in predicting pathological complete response (pCR) across molecular subtypes, data from Southeast Asian populations, including Thailand, remain limited. In this region, the

majority of patients present with heterogeneously dense to extremely dense breast tissue, which may impact imaging outcomes. Furthermore, differences in tumor biology, imaging interpretation, access to diagnostic technology, and treatment protocols may influence the diagnostic performance and reliability of MRI in this specific context. The scarcity of locally relevant evidence underscores the need for region-specific validation of imaging strategies in the neoadjuvant setting.

This study aims to evaluate the concordance between preoperative imaging modalities— MRI and US—and final pathological findings in breast cancer patients undergoing NAST at Siriraj Hospital. Additionally, patterns of tumor shrinkage (concentric vs. scattered) are characterized according to molecular subtype to inform surgical decision-making. The findings are expected to provide insight into the reliability of current imaging strategies for predicting residual disease and support evidence-based surgical planning in the neoadjuvant setting.

MATERIALS AND METHODS

Study design

This retrospective observational study was conducted at Siriraj Hospital and Siriraj Piyamaharajkarun Hospital in Bangkok, Thailand, with ethical approval from the Siriraj Institutional Review Board.

Patient selection

Female patients with histologically confirmed breast cancer who received NAST followed by surgery between January 2016 and December 2024 were reviewed.

Inclusion criteria:

1. Age ≥18 years
2. Receipt of NAST (chemotherapy, targeted therapy, or immunotherapy)
3. Availability of preoperative MRI and US within 3–6 weeks before surgery
4. Complete histopathological report from surgery

Exclusion criteria:

1. MRI performed at outside institutions
2. Incomplete imaging or pathology records

Out of 196 breast cancer patients reviewed: 156 did not receive NAST, 8 lacked post-NAST MRI, 6 lacked post-NAST ultrasound for comparison, and 2 had incomplete clinical or imaging data, as shown in Fig 1. Ultimately, 24 patients were included in the study.

Imaging technique and imaging analysis

Imaging protocols were standardized. Breast MRI included axial T1-weighted (T1W) and sagittal T2-weighted (T2W) fat-suppressed sequences, diffusion-weighted imaging (DWI), and post-contrast dynamic series using

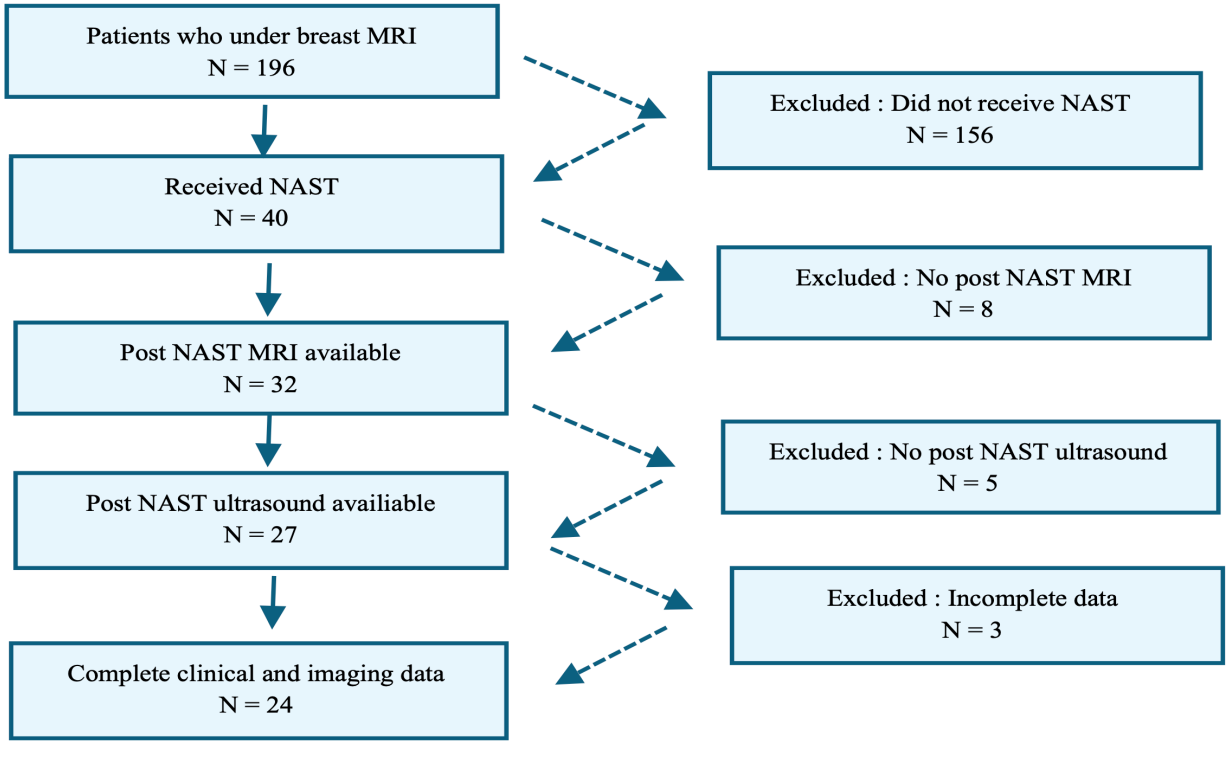

Fig 1. The chart illustrates the patient recruitment flow in this study.

gadolinium. Only measurable mass lesions were used for primary tumor size estimation; NME was recorded but excluded from initial measurements. Ultrasound was performed using high-resolution linear-array transducers and interpreted by board-certified radiologists.

To ensure reliability and minimize interpretive bias, two board-certified breast radiologists independently reviewed the MRI scans, blinded to the surgical pathology results. In cases demonstrating non-mass enhancement (NME), the maximal linear extent was measured in millimeters using dynamic contrast-enhanced sequences. Inter-observer agreement demonstrated substantial reliability, with an intraclass correlation coefficient (ICC) of 0.67. According to standard interpretation criteria, ICC values between 0.61 and 0.80 are indicative of substantial agreement.

With regard to tumor response patterns following neoadjuvant systemic therapy (NAST), two distinct types were identified: concentric shrinkage as demonstrated in Fig 2A and 2B and scattered shrinkage, as shown in Fig 3A and 3B. These patterns were documented and analyzed in relation to the molecular subtypes of breast cancer to assess potential correlations.

Data collected included age, tumor histology and subtype, imaging findings, type of surgery, and pathologic tumor size. Molecular subtypes were categorized as HER2-enriched, TNBC, or luminal B, based on immunohistochemistry and DISH results.

Statistical analysis

Descriptive statistics were used for mean, standard deviation (SD), median, minimum, maximum, and range.

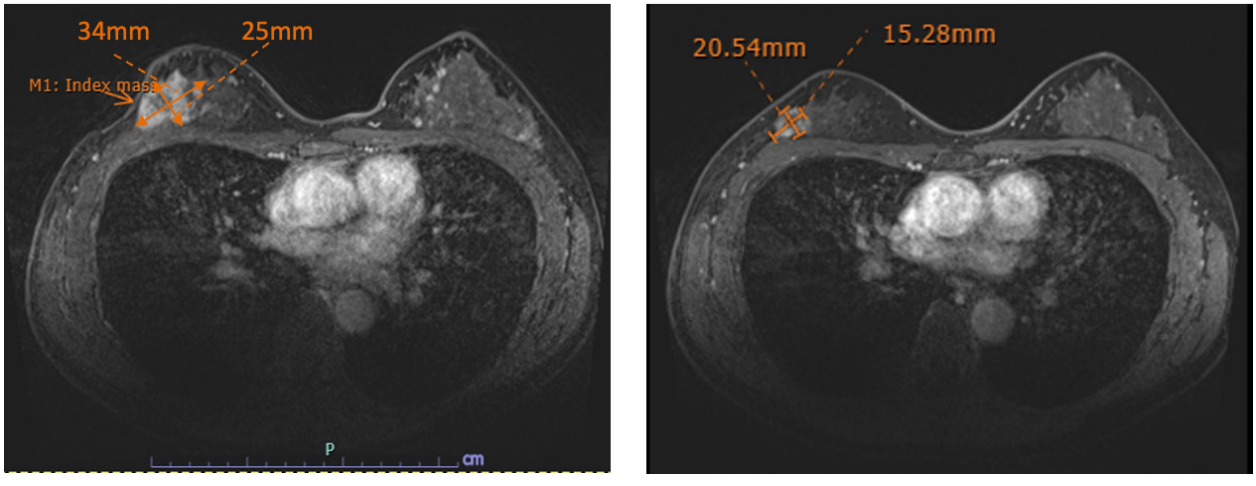

A B

Fig 2. Concentric shrinkage response on MRI. Fig 2A and 2B demonstrate MRI at initial diagnosis and after completion of NAST, respectively.

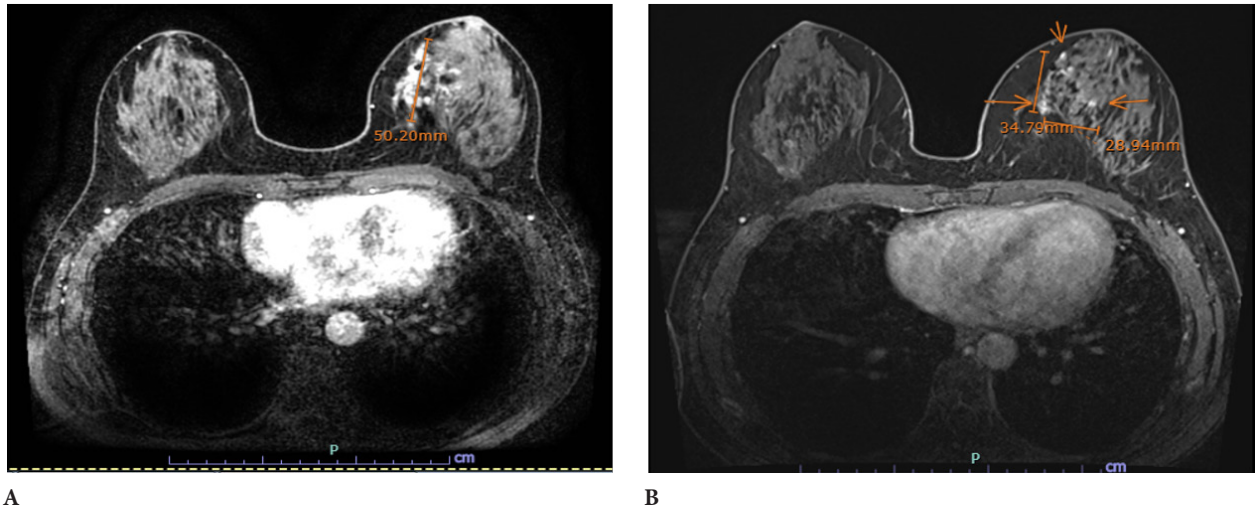

A B

Fig 3. Scattered shrinkage response on MRI. Fig 3A and 3B depict MRI scans at initial diagnosis and following completion of NAST, respectively.

Crosstabulation analysis was conducted to evaluate categorical agreement between imaging-based tumor size categories and was expressed as the proportion (%) of correctly classified cases. Bland-Altman plots were used to assess agreement between imaging and pathology. Statistical analyses were performed using SPSS version 29.

RESULTS

A total of 24 patients were initially identified, as shown in Table 1. All patients received neoadjuvant systemic treatment based on their cancer subtypes prior to surgery. Regarding surgical treatment, 62.5% (n = 15) of patients underwent wide excision, while 37.5% (n = 9) underwent mastectomy, including modified radical mastectomy (MRM), nipple-sparing mastectomy (NSM), and total mastectomy (TM). Non-mass enhancement (NME) on preoperative MRI was observed in 37.5% (n = 9) of patients, while the remaining 62.5% (n = 15) showed no evidence of NME. Following neoadjuvant treatment, the predominant tumor shrinkage pattern observed on MRI was concentric mass shrinkage, present in 83.3% (n = 20) of patients. In contrast, a scattered or NME shrinkage pattern was identified in 16.7% (n = 4). The tumor dimensions reported on MRI, ultrasound (US), and pathology were based on the longest diameter of the lesion.

Table 2 presents the distribution of tumor shrinkage patterns according to molecular subtype. Concentric shrinkage was observed in the majority of cases (83.3%), while scattered shrinkage was identified in 16.7%. Among patients with triple-negative breast cancer (TNBC), 72.7% exhibited a concentric shrinkage pattern, whereas scattered shrinkage was observed in 3 of 11 cases (27.3%). In the luminal B HER2-negative group, 83.3% demonstrated concentric shrinkage. Notably, all cases in the luminal B HER2-positive and HER2-overexpressing subtypes exhibited concentric shrinkage exclusively. Although descriptive trends suggest that HER2-driven tumors and luminal B subtypes are more likely to exhibit concentric shrinkage patterns, statistical analysis did not reveal a significant association between molecular subtype and shrinkage pattern (p = 0.646), which may, in part, be attributed to the limited sample size.

To evaluate clinical agreement between imaging modalities and pathological tumor size, a predefined threshold of ±10 mm was applied. MRI demonstrated high overall agreement with pathological measurements, with 91.7% of cases falling within the ±10 mm threshold. Only two patients (8.3%) exceeded this threshold, both of whom had invasive lobular carcinoma (ILC), a subtype known for its diffuse growth and less distinct imaging characteristics. In contrast, US measurements deviated by more than ±10 mm in 7 patients (29.1%), indicating

TABLE 1. Demographic data for all 24 patients recruited in the study—including breast cancer subtype, type of breast surgery, presence of NME on pre-NAST MRI, and shrinkage pattern on post-NAST MRI prior to surgery.

Characteristic	N = 24 (%)
Subtype	
Triple-negative (TNBC)	11 (45.8%)
Luminal B HER2 negative	6 (25%)
Luminal B HER2 positive	4 (16.7%)
HER2 overexpression	3 (12.5%)
Surgery Type	
Wide excision (WE)	15 (62.3%)
Mastectomy (MRM, NSM, TM)	9 (37.5%)
Presence of NME on MRI	
Yes	9 (37.5%)
No	15 (62.5%)
Shrinkage Pattern in MRI	
Concentric	20 (83.3%)
Scattered	4 (16.7%)

Abbreviations: TNBC – triple-negative breast cancer, WE – wide excision, MRM – modified radical mastectomy, NSM – nipple-sparing mastectomy, TM – total mastectomy, NME – non-mass enhancement

TABLE 2. Distribution of tumor shrinkage patterns by molecular subtype in breast cancer patients following NAST. The table summarizes the frequency of concentric and scattered shrinkage patterns across molecular subtypes. While concentric shrinkage was predominant overall, variation was observed among subtypes.

Subtype	Concentric shrinkage	Scattered shrinkage
Triple-negative	8	3
Luminal B HER2 negative	5	1
Luminal B HER2 positive	4	0
HER2 overexpression	3	0

a greater discrepancy compared to MRI and a higher likelihood of both underestimation and overestimation compared to pathology. Table 3 summarizes the mean, median, and standard deviation of tumor sizes as measured by MRI, US, and pathological examination.

These results suggest that MRI provides a more accurate and reliable estimation of residual tumor size following neoadjuvant treatment, whereas US may be more prone to underestimation or overestimation, particularly in tumors with diffuse growth patterns, such as invasive lobular carcinoma.

According to the Bland–Altman plots presented in Fig 4, MRI and US demonstrated differing levels of agreement with pathological tumor size following neoadjuvant treatment. For MRI (Fig 4.1), the mean difference between pathological and MRI measurements was +5.5 mm, indicating a slight tendency for MRI to overestimate tumor size. The limits of agreement ranged from –23.5 mm to +34.5 mm, reflecting moderate variability. Most measurements clustered near the mean, with only two data points falling outside the 95% confidence limits—both corresponding to cases of invasive lobular carcinoma (ILC), a subtype characterized by diffuse growth and ill-defined imaging features. The 95% confidence interval (CI) for the mean difference was –0.7 to 11.7 mm.

In contrast, the US Bland–Altman plot (Fig 4.2) revealed greater variability. Although the mean difference was slightly lower at +2.6 mm, the limits of agreement were considerably wider (–32.8 mm to +38.0 mm), indicating lower consistency and weaker agreement with pathological measurements. The 95% CI for the mean difference was –5.0 to 10.2 mm.

The difference in agreement between MRI and US in estimating residual tumor size was not statistically significant at the conventional $\alpha = 0.05$ level; however, a trend toward significance was observed, with a two-sided

TABLE 3. Comparison of tumor size measurements by imaging modality and pathology.
Mean, median, and standard deviation of lesion size as determined by MRI, US, and pathological examination. The proportion of cases exceeding a ±10 mm discrepancy from pathological tumor size is also reported as the percentages.

Modality	Mean Tumor Size (mm)	Standard Deviation (SD)	Accuracy within 10 mm
MRI	5.4 (0-20.5)	6.34	91.67%
Ultrasound	8.3 (0-25.4)	8.1	70.83%
Pathological Report	10.9 (0-25.0)	16.1	

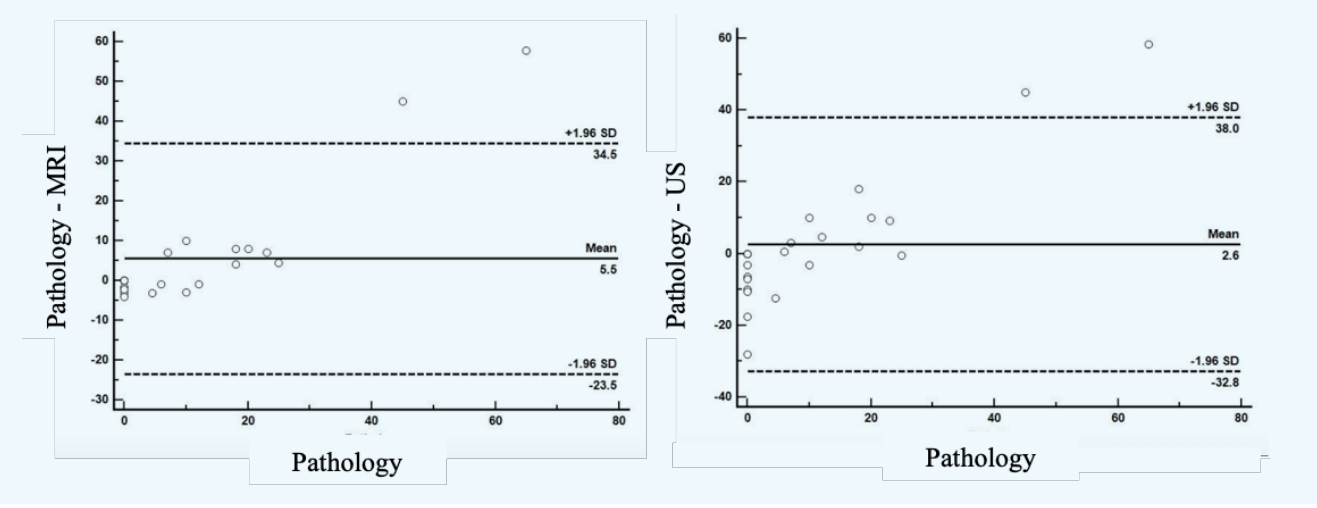

Fig 4.1 Fig 4.2

Fig 4. Bland–Altman analysis of agreement between imaging modalities and pathological tumor size following NAST in all 24 patients. Fig 4.1: Bland–Altman plot comparing MRI measurements with pathological tumor size. Fig 4.2: Bland–Altman plot comparing US measurements with pathological tumor size.

p-value of 0.081 for the comparison between MRI and pathological measurements. In contrast, the US–pathology comparison yielded a non-significant p-value of 0.489.

Notably, when the two cases of invasive lobular carcinoma (ILC) were excluded from the analysis, MRI demonstrated minimal bias (mean difference = 1.3 mm) with narrow limits of agreement (–7.0 mm to +9.6 mm), indicating good concordance with pathological measurements. The 95% confidence interval (CI) for the mean difference was –0.53 to 3.21 mm.

Conversely, ultrasound (US) exhibited greater bias (mean difference = –1.9 mm) and wider limits of agreement (–21.7 mm to +17.9 mm), reflecting increased variability and reduced agreement with pathology, as illustrated in Figure 5. The 95% confidence interval (CI) for the mean difference was –6.3 to 2.5 mm.

Subgroup analysis by tumor size category

To further evaluate diagnostic performance according to tumor size, patients were stratified into two groups based on pathological tumor size: < 10 mm. and ≥ 10 mm.

Among the 14 patients with tumors < 10 mm. on pathology, MRI correctly classified all cases, yielding a concordance rate of 100.0%. In the ≥ 10 mm. group (n = 10), MRI accurately identified seven patients (70.0%),

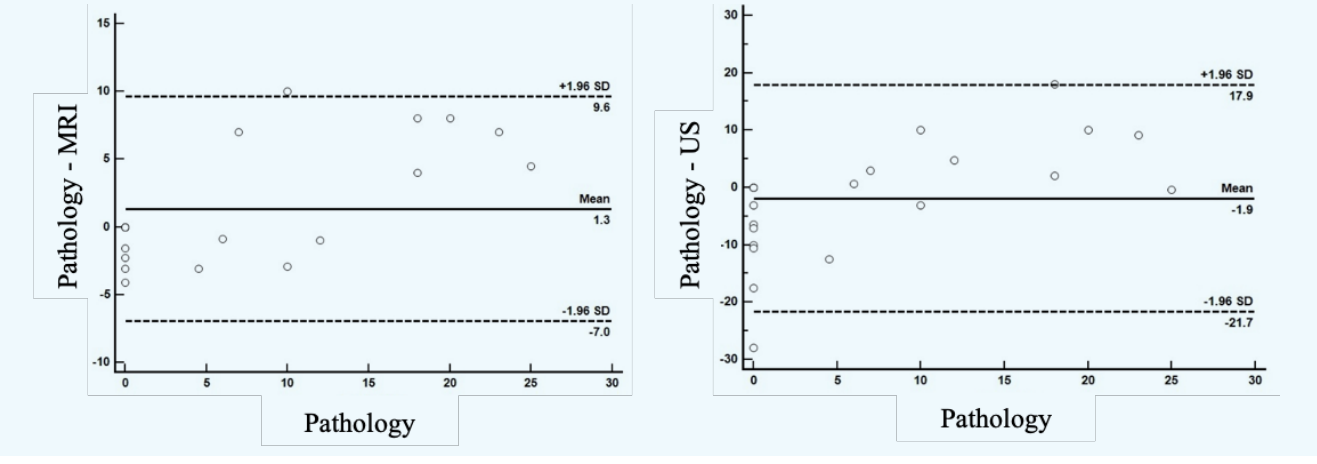

Fig 5.1 Fig 5.2

Fig 5. Bland–Altman analysis of agreement between imaging modalities and pathological tumor size after exclusion of invasive lobular carcinoma (ILC) cases. Fig 5.1: Bland–Altman plot comparing MRI with pathological tumor size. Fig 5.2: Bland–Altman plot comparing US with pathology. The plots demonstrate that MRI exhibits closer agreement with pathology, with lower bias and narrower limits of agreement compared to US.

with three cases underestimated as < 10 mm. (30.0%). In contrast, ultrasound showed lower concordance with pathological findings. Among patients with tumors < 10 mm., nine of 14 cases (64.3%) were correctly classified, while five cases were misclassified. In the ≥ 10 mm. group, five of ten cases (50.0%) were correctly identified. These findings correspond to classification accuracies of 64.3% for tumors < 10 mm and 50.0% for tumors ≥ 10 mm using ultrasound.

The comparative analysis of MRI and US in estimating residual tumor burden following NAST demonstrated superior consistency and accuracy of MRI in correlation with final pathological measurements. In the full cohort (N = 24), the correlation between MRI and pathology approached statistical significance ($r = 0.401$, $p = 0.052$), with a mean paired difference of 5.51 mm ($p = 0.081$) and a moderate effect size (Cohen's $d = 0.372$). In contrast, US demonstrated negligible correlation with pathological tumor size ($r = 0.005$, $p = 0.983$) and exhibited greater variability in size estimation.

Of particular interest, when two cases of invasive lobular carcinoma were excluded from the analysis (N = 22), the correlation between MRI and pathology improved substantially ($r = 0.882$, $p < 0.001$). However, the corresponding mean difference and effect size were reduced and did not reach statistical significance (mean difference $p = 0.152$, Cohen's $d = 0.317$). These findings suggest that specific tumor subtypes—particularly ILC, which is characterized by a diffuse growth pattern and a tendency to present as non-mass enhancement (NME) on MRI—may limit the accuracy and reliability of MRI-based tumor size estimation.

The stronger correlation observed in the complete dataset may better reflect the heterogeneity encountered in routine clinical practice. Therefore, while MRI remains a valuable modality for preoperative assessment, its interpretation should be contextualized with respect to tumor biology and imaging phenotype, particularly in histologic subtypes such as ILC, where diffuse growth patterns may lead to underestimation. Overall, MRI consistently demonstrated superior agreement with pathological tumor size compared to US, regardless of tumor dimension, supporting its greater accuracy in preoperative tumor evaluation following neoadjuvant therapy.

DISCUSSION

This study demonstrates the superior accuracy of breast magnetic resonance imaging (MRI) compared to ultrasound (US) in assessing residual tumor size following neoadjuvant systemic therapy (NAST) in patients with breast cancer. Notably, MRI maintained measurement accuracy within ±10 mm of pathological size in 91.7% of cases—a clinically meaningful threshold in surgical planning, particularly for ensuring adequate oncologic margins while enabling breast-conserving approaches. In contrast, US overestimated tumor size by more than 10 mm in seven cases and underestimated it in one case. These findings highlight the greater consistency and precision of MRI in the preoperative evaluation of residual disease.

Our data further indicate that MRI provided narrower limits of agreement and more accurate tumor size classification than US. This advantage was especially evident in lesions smaller than 10 mm., where precise measurements are critical for evaluating breast-conserving surgery (BCS) feasibility and ensuring appropriate margin clearance. Importantly, in cases of ILC, conventional MRI techniques focusing solely on mass-forming lesions tended to underestimate disease extent. Incorporating non-mass enhancement (NME) into radiologic assessment substantially improved correlation with pathological findings. This aligns with prior reports suggesting that the diffuse infiltration pattern and low cellularity of ILC require a tailored imaging approach that considers both mass and NME characteristics. Future imaging protocols should thus integrate comprehensive assessment strategies, particularly for lobular and low-grade tumors.

Accurate preoperative imaging is crucial not only for optimizing surgical strategy but also for reducing reoperation rates and minimizing the risk of local recurrence or distant metastasis. Although multiple imaging modalities are used to assess residual disease post-NAST, no single technique has yet been established as the gold standard. First-line options such as mammography and US are limited by factors including breast density, resolution, and operator dependency—challenges that are further compounded post-NAST due to altered tumor morphology. While lesions ≥ 7 mm are more reliably detected, overall accuracy remains moderate, typically ranging from 60% to 80%.[9]

Automated breast ultrasound (ABUS) provides a standardized, operator-independent approach with multiplanar imaging capabilities. Reported diagnostic metrics for ABUS include a sensitivity of 22.2%, specificity of 95.2%, positive predictive value (PPV) of 50.0%, and negative predictive value (NPV) of 85.1%.[10] Digital breast tomosynthesis (DBT), which addresses the tissue overlap limitations of 2D mammography, improves delineation of tumor margins. For prediction of pathological complete response (pCR), DBT has shown a sensitivity of 44.7%, specificity of 97.6%, PPV of 85.7%, and NPV of 93.2%.[11-14]

Contrast-enhanced mammography (CEM), which combines dual-energy acquisition with iodinated contrast, serves as a valuable adjunct when standard mammography is inconclusive, with reported sensitivity, specificity, and accuracy of 81%, 83%, and 82%, respectively.

MRI has increasingly been adopted for preoperative assessment due to its high sensitivity and superior soft-tissue contrast. One study reported MRI sensitivity, specificity, and accuracy for residual disease detection at 100%, 86%, and 90%, respectively. In direct comparison, Bernardi et al. found MRI significantly more sensitive than CEM in detecting pCR.[15] A systematic review reported a median MRI sensitivity of 42%, specificity of 89%, PPV of 64%, and NPV of 87%.[16] In a meta-analysis of 25 studies, Yuan et al. reported pooled MRI sensitivity and specificity for predicting pCR of 63% (95% CI: 56–70%) and 91% (95% CI: 89–92%), respectively.[17] However, despite its strengths, MRI remains susceptible to false positives, which may lead to overtreatment or unnecessary mastectomy.

International guidelines support the use of MRI in this context. The European Society of Breast Cancer Specialists (EUSOMA) recommends pre-NAST MRI for patients considered for BCS, to better evaluate tumor extent and breast anatomy. Likewise, the American College of Radiology (ACR) recognizes MRI as the most specific modality for assessing residual disease and post-treatment breast changes. This is particularly relevant in Asian populations, where dense breast tissue poses a challenge for mammographic interpretation.[18] MRI has been shown to outperform both mammography and US in lesion detection,[19-23] and uniquely identifies multifocal or multicentric disease, non-mass lesions, contralateral synchronous tumors, and tumor shrinkage patterns—all of which are critical in guiding surgical decisions.

Although MRI demonstrates greater accuracy in estimating tumor extent compared to US, US remains clinically valuable in routine practice. Its advantages include broader accessibility, lower cost, and the capability for real-time, dynamic assessment at the point of care. These features make US particularly useful in resource-limited settings or among patients who are not suitable candidates for MRI. In addition, US provides complementary information—such as lesion vascularity and tissue elasticity—that can aid in the characterization of indeterminate findings.

From a surgical standpoint, inaccurate estimation of tumor extent on imaging can have direct implications for operative planning. Overestimation may result in unnecessarily wide excision or mastectomy, whereas underestimation increases the risk of positive margins and subsequent reoperation. In a study by Thiravit et al.[24], MRI maintained high diagnostic accuracy across different levels of background parenchymal enhancement (BPE), with accuracy rates of 84.4% in minimal-to-mild BPE and 73.3% in moderate-to-marked BPE, with no statistically significant difference observed ($p = 0.35$). These findings suggest that preoperative MRI can accurately evaluate tumor extent in breast cancer, and that moderate-to-marked background enhancement does not significantly impact its performance.

Several limitations of this study must be acknowledged. Its retrospective nature limits causal inference and introduces potential selection bias. The sample size was modest, restricting the power of subgroup analyses, particularly among luminal and lobular subtypes. Moreover, interobserver variability in the interpretation of NME was not formally evaluated, although a second blinded review by an experienced radiologist confirmed consistency with initial reports.

Future prospective studies with larger, subtype-stratified cohorts are needed to validate these findings. Standardized radiologic response criteria that incorporate both mass and NME characteristics may enhance consistency across institutions. Furthermore, integrating advanced functional MRI techniques—such as diffusion-weighted imaging (DWI) and dynamic contrast-enhanced (DCE) sequences—could refine evaluation of post-NAST residual disease, particularly in non-pCR cases.

In summary, our findings affirm the diagnostic value of MRI in evaluating post-NAST residual disease and emphasize the need to integrate tumor biology into radiologic interpretation. With further validation, preoperative breast MRI should be established as a key component of surgical planning for selected breast cancer patients, particularly when conventional imaging modalities are likely to underperform.

CONCLUSION

This study demonstrates that breast MRI provides superior accuracy compared to US in evaluating residual tumor burden following neoadjuvant systemic therapy, particularly in HER2-positive, triple-negative, and subcentimeter tumors. MRI enhances surgical planning by improving preoperative tumor size estimation and reducing the likelihood of positive surgical margins. In the context of breast-conserving surgery, accurate imaging is critical in determining surgical eligibility and supports treatment decisions that are both oncologically sound and aligned with patient preferences.

The findings also highlight important considerations in specific tumor subtypes. Invasive lobular carcinoma

and certain luminal tumors often present with non-mass enhancement that may not be captured through conventional measurement criteria. Integrating these imaging patterns into preoperative assessment may prevent underestimation of disease extent and reduce the likelihood of inadequate resections.

Given these clinical implications, use of preoperative MRI should be considered in patients undergoing neoadjuvant therapy, especially when imaging findings will critically inform surgical decision-making. Incorporating tumor biology and response patterns into radiologic interpretation is not only diagnostically advantageous but also essential in tailoring surgery to the individual patient.

However, several limitations must be acknowledged, including the retrospective study design and relatively small sample size. Therefore, while the findings support the clinical utility of MRI in this context, prospective studies are warranted to validate these results before routine implementation in all clinical settings.

Data Availability Statement

The datasets generated and/or analyzed during the current study include patient information and medical imaging, which are subject to ethical and legal restrictions. As such, these data are not publicly available. De-identified data may be made available from the corresponding author upon reasonable request and with approval from the Siriraj Institutional Review Board.

ACKNOWLEDGEMENT

The authors gratefully acknowledge Ms. Julaporn Pooliam, M.Sc., Research Department, Faculty of Medicine Siriraj Hospital, Mahidol University, for her valuable support in statistical advice and analysis.

DECLARATIONS

Grants and Funding Information

None.

Conflict of Interest

None.

Registration Number of Clinical Trial

No due to retrospective observational study.

Author Contributions

Conceptualization and methodology, A.I., P.K., S.C., and W.I. ; Investigation, A.I., S.T., V.S., P.R., W.I. ; Formal analysis, A.I. and W.I. ; Visualization and writing – original draft, A.I. ; Writing – review and editing, W.I. ; Funding acquisition, A.I. and W.I.; Supervision, W.I. All authors have read and agreed to the final version of the manuscript.

Use of Artificial Intelligence

None.

REFERENCES

1. ทะเบียนมะเร็งระดับโรงพยาบาล พ.ศ. 2564 สถาบันมะเร็งแห่งชาติกรมการแพทย์กระทรวงสาธารณสุข, www.nci.go.th/e_book/hosbased_2564/index.html
2. Cortazar P, Zhang L, Untch M, Mehta K, Costantino JP, Wolmark N, et al. Pathological complete response and long term clinical benefit in breast cancer: the CTNeoBC pooled analysis. Lancet. 2014;384:164-72.
3. Zheng C-H, Xu K, Shan W-P, Zhang Y-K, Su Z-D, Gao X-J, et al. Meta-Analysis of Shrinkage Mode After Neoadjuvant Chemotherapy for Breast Cancers: Association With Hormonal Receptor. Front Oncol. 2022;11:617167.
4. Negarao EMS, Souza JA, Marques EF. Breast cancer phenotype influences MRI response evaluation after neoadjuvant chemotherapy. Eur J Radiol. 2019;120:108701.
5. Price ER, Wong J, Mukhtar R, Hylton N, Esserman LJ. How to use magnetic resonance imaging following neoadjuvant chemotherapy in locally advanced breast cancer. World J Clin Cases. 2015;3(7):607-13.
6. Boughey JC, McCall LM, Ballman KV, Mittendorf EA, Ahrendt GM, Wilke LG, et al. Tumor Biology Correlates With Rates of Breast-Conserving Surgery and Pathologic Complete Response After Neoadjuvant Chemotherapy for Breast Cancer: Findings From the ACOSOG Z1071 (Alliance) Prospective Multicenter Clinical Trial. Ann Surg. 2014; 260(4):608–16.
7. JEON-HOR CHEN. Impact of Factors Affecting the Residual Tumor Size Diagnosed by MRI Following Neoadjuvant Chemotherapy in Comparison to Pathology. J Surg Oncol. 2014;109(2):158-67.
8. Kim J, Han B, Ko E, Ko E, Choi J, Park K. Prediction of pathologic complete response on MRI in patients with breast cancer receiving neoadjuvant chemotherapy according to molecular subtypes. Eur Radiol. 2022;32(6):4056-66.
9. Croshaw R, Shapiro-Wright H, Svensson E, Erb K, Julian T. Accuracy of clinical examination, digital mammogram, ultrasound, and MRI in determining postneoadjuvant pathologic tumor response in operable breast cancer patients. Ann Surg Oncol. 2011;18:3160-3.
10. Jiyoon Park, Eun Young Chae, Jo Hee Cha, Hee Jung Shin, Woo Jung Choi, Young-Wook Choi, et al. Comparison of mammography, digital breast tomosynthesis, automated T breast ultrasound, magnetic resonance imaging in evaluation of residual tumor after neoadjuvant chemotherapy. Eur J Radiol. 2018;108:261–8.
11. Poplack SP, Tosteson TD, Kogel CA, Nagy HM. Digital breast tomosynthesis: initial experience in 98 women with abnormal digital screening mammography. AJR Am J Roentgenol. 2007;189(3): 616–23.
12. Fornvik D, Zackrisson S, Ljungberg O, Svahn T, Timberg P, Tingberg A, Andersson I. Breast tomosynthesis: accuracy of tumor measurement compared with digital mammography and ultrasonography. Acta Radiol. 2010;51(3):240–7.

13. Hakim CM, Chough DM, Ganott MA, Sumkin JH, Zuley ML, Gur D. Digital breast tomosynthesis in the diagnostic environment: a subjective side-by-side review. AJR Am. J Roentgenol. 2010; 195:W172–6.
14. Park JM, Franken Jr. EA, Garg M, Fajardo LL, Niklason LT. Breast tomosynthesis: present considerations and future applications. Radiographics. 2007;27 Suppl 1:S231–S40.
15. Bernardi D, Vatteroni G, Acquaviva A, Valentini M, Sabatino V, Bolengo I, et al. Contrast-Enhanced Mammography Versus MRI in the Evaluation of Neoadjuvant Therapy Response in Patients With Breast Cancer: A Prospective Study. AJR Am J Roentgenol. 2022;219(6):884–94.
16. Lobbes MBI, Previous R, Smidt M, Tjan-Heijnen VCG, van Goethem M, Schipper R, et al. The role of magnetic resonance imaging in assessing residual disease and pathologic complete response in breast cancer patients receiving neoadjuvant chemotherapy: a systematic review. Insights Imaging. 2013; 4(2):163–75.
17. Yuan Y, Chen X-S, Liu S-Y, Shen K-W. Accuracy of MRI in prediction of pathologic complete remission in breast cancer after preoperative therapy: a meta-analysis. AJR Am J Roentgenol. 2010;195(1):260– 8.
18. Marinovich ML, Houssami N, Macaskill P, Sardanelli F, Irwig L, Mamounas EP, et al. Meta-analysis of Magnetic Resonance Imaging in Detecting Residual Breast Cancer After Neoadjuvant Therapy. J Natl Cancer Inst. 2013;105:321–33.
19. França LKL, Bitencourt AGV, Paiva HLS, Silva CB, Pereira NP, Paludo J, et al. Role of magnetic resonance imaging in the planning of breast cancer treatment strategies: comparison with conventional imaging techniques. Radiol Bras. 2017;50(2):76–81.
20. França LKL, Bitencourt AGV, Osório VAB, Graziano L, Guatelli CS, Souza JA, et al. Tumor size assessment of invasive breast cancers: which pathological features affect MRI-pathology agreement. Applied Cancer Research. 2018;38:2.
21. Ko ES, Han BK, Kim RB, Ko EY, Shin JH, Hahn SY, et al. Analysis of Factors That Influence the Accuracy of Magnetic Resonance Imaging for Predicting Response after Neoadjuvant Chemotherapy in Locally Advanced Breast Cancer. Ann Surg Oncol. 2013; 20:2562–8.
22. Bahri S, Chen JH, Mehta RS, Carpenter PM, Nie K, Kwon S, et al. Residual Breast Cancer Diagnosed by MRI in Patients Receiving Neoadjuvant Chemotherapy with and Without Bevacizumab. Ann Surg Oncol. 2009;16:1619–28.
23. Kim HJ, Im YH, Han BK, Choi N, Lee J, Kim JH, et al. Accuracy of MRI for Estimating Residual Tumor Size after Neoadjuvant Chemotherapy in Locally Advanced Breast Cancer: Relation to Response Patterns on MRI. Acta Oncol Stockh Swed. 2007;46: 996–1003.
24. Thiravit S. The Background Parenchymal Enhancement in Preoperative Breast MRI: The Effect on Tumor Extent Evaluation. Siriraj Med J. 2017;69(5):290-6.